Exosomal MicroRNA Profiling in Vitreous Humor Derived From Pathological Myopia Patients

Jie You,[1–3] Qiao Wu,[4,5] Gezhi Xu,[1–3] Chenyang Gu,[1–3] Edward Allen,[6] Tianrui Zhu,[7] and Ling Chen[1–3]

[1]Department of Ophthalmology & Vision Science, Eye & ENT Hospital, Shanghai Medical School, Fudan University, Shanghai, China
[2]Key NHC Key Laboratory of Myopia (Fudan University), Laboratory of Myopia, Chinese Academy of Medical Sciences, Shanghai, China
[3]Shanghai Key Laboratory of Visual Impairment and Restoration, Eye & ENT Hospital, Shanghai Medical School, Fudan University, Shanghai, China
[4]Department of General Surgery, Zhongshan Hospital, Fudan University, Shanghai, China
[5]School of Life Sciences, Fudan University, Shanghai, China
[6]Institute of Archaeological Science, Fudan University, Shanghai, China
[7]University of Washington, Seattle, Washington, United States

Correspondence: Ling Chen, Department of Ophthalmology & Vision Science, Eye & ENT Hospital, Fudan University, Shanghai, China; linglingchen98@hotmail.com.

Received: April 26, 2022
Accepted: December 8, 2022
Published: January 17, 2023

Citation: You J, Wu Q, Xu G, et al. Exosomal microRNA profiling in vitreous humor derived from pathological myopia patients. *Invest Ophthalmol Vis Sci.* 2023;64(1):9. https://doi.org/10.1167/iovs.64.1.9

Purpose. Pathologic myopia (PM) is one of the primary causes of blindness. This study aims to explore the possible relations between the composition of microRNA in vitreous exosomes of patients with PM and the progression of myopic maculopathy.

Methods. Vitreous humor (VH) samples were collected from patients undergoing retinal surgery. A total of 15 and 12 VH samples were obtained from patients with PM and control, respectively. The PM group was divided into PM-L (G2) and PM-H groups (G3 and G4) in order to explore differentially expressed microRNAs (DEMs) that account for the relatively poor prognosis in G3 and G4 myopic maculopathy. A Weighted Gene Co-Expression Network Analysis (WGCNA) was conducted to find the persistently altered key microRNAs in myopic maculopathy progression. The Gene Ontology (GO) enrichment analysis and Kyoto Encyclopedia of Genes and Genome (KEGG) pathway enrichment analysis were used.

Results. High purity exosomes were extracted from the vitreous fluid of patients with PM and control. The top five downregulated DEMs of PM-H versus PM-L can reflect the tendency of deterioration of PM-H myopic maculopathy. *MiR-143-3p* and *miR-145-5p*, which were found in WGCNA, may participate in the development of myopic maculopathy. These microRNAs all relate to the insulin resistance pathway.

Conclusions. This is the first study to explore the relations between the progression of myopic maculopathy and vitreous exosomal microRNAs. Vitreous exosomal *miR-143-3p* and *miR-145-5p* can be considered biomarkers for patients with PM, and the vitreous exosomal DEM associated with PM-H may represent alarming signals of myopic maculopathy deterioration.

Keywords: pathological myopia (PM), myopic maculopathy, exosome, microRNA, vitreous humor (VH)

By 2050, it is estimated that nearly half of the world's population will suffer from myopia, among which 10% will be highly myopic.[1] Pathological myopia (PM) is the term for a form of myopia with excessive axial elongation that leads to structural changes in the posterior segment of the eye (including posterior staphyloma, myopic maculopathy, and high myopia-associated optic neuropathy) and that can lead to loss of best corrected visual acuity.[2] This is one of the main causes of blindness and poor vision in 12% to 27% of the Asian population.[3] Due to the difficulties in obtaining retinal tissues from patients with PM, few researchers have explored the causes and the mechanism underlying myopic maculopathy.

The exosome, a kind of extracellular vesicle (EV) features a double-membrane structure and an average diameter of 30 to 150 nm, and contains several cell-specific proteins, lipids, mRNA, and microRNA that play important roles in cell communication, anti-apoptosis, and immune regulation.[4] MicroRNAs and proteins in aqueous humor exosomes differentiate between patients with high myopia and non-myopia.[5,6] It has been reported that exosomes secreted by mesenchymal stem cells and neural progenitor cells can protect retinal photoreceptors and combat retinal degeneration through a variety of microRNA.[7,8] In this way, exosomal microRNAs may play an important role in myopic maculopathy. Exosomes are widely found in the extracellular matrix

and have been confirmed to exist in VH. Because the vitreous body does not contain any cell structures, exosomes in the posterior vitreous body are mainly derived from the retinal epithelium and vascular endothelium.[9] Progression of myopic maculopathy may be indirectly reflected by components of vitreous exosomes.

We hypothesized that vitreous and exosomal microRNAs in patients with PM may be involved in the development of myopia maculopathy by regulating targeted genes as well as the function and metabolism of adjacent or distant tissues. This study aims to explore the possible associations of microRNAs in vitreous exosomes of patients with PM and the progression of myopic maculopathy using next-generation sequencing (NGS) technology and bioinformatics analysis.

Materials and Methods

Patients and VH Samples

This study was approved by the Institutional Review Board of the Eye & ENT Hospital of Fudan University and adhered to the tenets of the Declaration of Helsinki. VH samples were collected from patients who met the selection criteria and underwent surgery for rhegmatogenous retinal detachment (RRD), idiopathic epiretinal membrane (ERM), myopic retinoschisis (MRS), and macular hole (MH) in the Eye & ENT Hospital of Fudan University between July 2020 and March 2021. Informed consent was obtained from all participants.

The PM group included surgically treated eyes with spherical equivalent refractive error (SRE) <-6 diopters (D), axial length (AL) >26.5 mm, and chorioretinal degeneration. Surgical treated eyes that had SRE >-6 D, AL <26.5 mm, and no chorioretinal degeneration were allocated to the control group. All patients were adults and went through comprehensive preoperative eye examinations (including visual acuity test, slit-lamp examination, indirect ophthalmoscopy, AL (IOLmaster 500; Carl Zeiss AG, Oberkochen, Germany), ophthalmic ultrasonography, and fundus optical coherence tomography) and medical history evaluation to rule out diabetic retinopathy, glaucoma, intravitreal injections, or history of internal ocular surgery, autoimmune retinal disease, history of eye trauma, or other conditions that may interfere with VH composition. The chorioretinal degeneration degree of all samples were determined according to a myopia maculopathy classification and grading system.[10] The baseline information of patients is provided in Table 1.

VH Samples. A sterile syringe (5 mL) was connected to the valve of the vitrector aspiration line. To minimize disturbance during follow-up retinal surgery, core VH diluted by sterile normal saline was aspirated into the 5 mL syringe before surgery by active vitrector cutting and syringe suction (25G; Constellation; Alcon Instruments, Fort Worth, TX, USA). This applied to all VH sample collections (PM and control groups). All VH samples (5 mL) were snap-frozen and stored at -80°C for further use.

Exosome Isolation. Exosome isolation was performed through ultracentrifugation. The stored VH sample was sequentially centrifuged at 4°C for 10 minutes at 300 g, 20 minutes at 2000 g, and 30 minutes at 10,000 g. The supernatant was ultracentrifuged at 4°C for 70 minutes at 100,000 g and the pellet was rinsed and resuspended in PBS. A highly purified exosome was obtained by a second ultracentrifugation at 100,000 g for 70 minutes at 4°C. The exosome preparation was passed through a 0.22 µm filter and stored at -20°C until use.

Characterization of Vitreous Exosomes

A nanoparticle tracking and NanoSight analysis (NTA) system was used to measure the amount and size distribution of exosomes (NS300; Malvern Instruments, Malvern, UK).

Western blotting (WB) analysis was conducted to determine positive and negative exosome surface markers. Briefly, total protein from exosomes was extracted in a lysis buffer and boiled at 95°C for 5 minutes. After SDS-PAGE electrophoresis (Tanon Science Inc., Shanghai, China), the lysates were transferred to 0.45 um polyvinylidene difluoride (PVDF) membranes and incubated with CD9 (Cat# ab223052, RRID: N/A), CD63 (Cat# ab134045, RRID: AB_2800495), CD81 (Cat# ab109201, RRID: AB_10866464), TSG101 (Cat# ab83, RRID: AB_306450), ACTB (Cat# ab8227, RRID: AB_2305186), Cytochrome C (Cat# ab133504, RRID: AB_2802115), and Calnexin (Cat# ab22595, RRID: AB_2069006) at 4°C overnight. All primary antibodies came from Abcam (Abcam plc., Cambridge, UK). The PVDF membranes were then incubated in the secondary antibody for 1 hour at room temperature, rinsed, and detected by chemiluminescence with HRP substrate (Merck KGaA, Darmstadt, Germany).

A transmission electron microscope (TEM) was used to observe the morphology of the exosome. The diluted exosome pallet was dropped onto copper grids and incubated at room temperature for 30 minutes. Negative staining

Table 1. Baseline Clinical Data of Included Eyes

Variables	Control ($n = 12$)	PM ($n = 15$)	P Value*
Age, y	60.83 ± 8.6	60.87 ± 7.8	0.992
Gender (M/F)	2/10	1/14	0.569
Diagnosis (n)	RRD ($n = 1$), MH ($n = 8$), ERM ($n = 3$)	RRD ($n = 1$), MH ($n = 7$), MRS ($n = 7$)	–
AL (mm)	23.2 ± 0.7	30.3 ± 1.8	<0.001
Grades of myopic maculopathy			
G0: no macular lesions	12	0	<0.001
G1: tessellated fundus	0	2 (13.3%)	
G2: diffuse chorioretinal atrophy	0	5 (33.3%)	
G3: patchy chorioretinal atrophy	0	7 (46.7%)	
G4: macular atrophy	0	1 (6.7%)	
Posterior staphyloma	0	15 (100%)	

* Student's t-test, PM, pathological myopia; AL, axial length.

Investigative Ophthalmology & Visual Science

was conducted by incubating 10 µL 2% tungsten phosphate solution (PH5.52) on the copper grids for 1 minute. After 15 minutes at room temperature, vesicles were observed with the TEM JEM1400 (JEOL Ltd., Tokyo, Japan) and photographed.

Extraction of Exosomal RNA. Total RNA was extracted from exosomes using a miRNeasy Micro Kit (Qiagen, Hilden, Germany), in accordance with the manufacturer's instructions. The highly sensitive Agilent 2100 PIC600 (Agilent Technology, Tokyo, Japan) was used to accurately detect the total amount and fragment distribution of RNA. RNA samples were then stored at −80°C prior to analysis.

VH Exosomal MicroRNA Sequencing and Bioinformatics Analyses

Only samples with a total RNA content >1 ng were involved in library establishment and RNA sequencing. TruSeq Small RNA Sample Preparation Kit (Illumina, San Diego, CA, USA) was used to establish the library. After cDNA synthesis, polymerase chain reaction (PCR) amplification and PAGE electrophoresis were used to separate and obtain the 0 to 150 bp target DNA fragment (0–22 nt microRNA). Qubit2.0, the detection of fragment distribution of the libraries, and QPCR were used to ensure library quality. Qualified libraries sequencing was performed using the Illumina Novaseq SE50 platform (Illumina) with a single-end 50 bp read length. Q20 and Q30 were applied as the quality control standard.

Raw reads were cleared, filtered, and normalized based on a published paper.[11] In short, sRNA with lengths between 19- and 28-nt were selected and mapped to the genome. Only reads that fail to match structural RNAs (rRNAs, tRNAs, snRNAs, and snoRNAs) were kept and used for downstream analysis. Normalized expression levels and differentially expressed analysis were calculated by DEGseq (version 1.50.0) package with CPM (counts per million) normalization.

To find out possible reasons underlying the relatively worse prognosis for the G3, G4 degree of myopic maculopathy compared with the G2 degree of myopic maculopathy, the PM group was further divided into PM-L (G2) and PM-H (G3 and G4) groups.

Fold changes in expression levels, P value (probability value), and false discovery rate (FDR; P value corrected using the Benjamini-Hochberg method) were calculated in PM versus control, PM-L versus control, PM-H versus control, and PM-H versus PM-L groups. DEM obtained were defined as those with a log2fold change $\geq$1.0 and $P < 0.01$.

To identify key microRNAs related to myopic maculopathy, A Weighted Gene Co-Expression Network Analysis (WGCNA) was conducted between the PM and control groups according to a previously described protocol.[12] Briefly, we measured the similarity between the gene expression profiles based on a matrix of pairwise Pearson's correlation coefficients. The similarity matrix was then transformed into an adjacency matrix using a power adjacency function. The power $\beta = 14$ was chosen based on the scale-free topology criterion, resulting in a scale-free topology index (R^2) of 0.86 (Supplementary Fig. S3). An average linkage hierarchical clustering with a dissimilarity measure was used to detect modules. The module eigengene was calculated and correlated with external traits. The Gene Significance (GS) and Module Membership (MM) were calculated for intramodular analysis. The node degree of a gene was evaluated and visualized using R (version 4.2.1).

The target genes of the differentiated expressed microRNAs (DEMs) and the module microRNAs were predicted using mirDIP version 5.2.2.1 (http://ophid.utoronto.ca/mirDIP/index.jsp). The GO (http://www.geneontology.org) enrichment analysis and Kyoto Encyclopedia of Genes and Genome (KEGG) pathway enrichment analysis were then used and graphically visualized by R. Cytoscape software version 3.9.1 (https://cytoscape.org/) was used to construct the predicted microRNA-mRNA network.

Statistical Analyses

Except for the bioinformation statistical analysis described above, data were expressed as mean ± standard error. Measurement data were treated with the Student's t-test and enumeration data was treated with the chi-square test using SPSS version 20 (SPSS Inc., Chicago, IL, USA). One-way analysis of variance was also calculated by SPSS. A P value < 0.05 indicated a statistically significant difference.

Results

Patient Characteristics

A total of 27 VH samples were collected from patients undergoing vitreoretinal surgery, including 12 samples from control patients and 15 samples from patients with PM (see Table 1). Fundus photographs of different grades of myopic maculopathy are shown in Figure 1.

Exosomes Exist in VH and Have Similar Characteristics to Exosomes From Other Body Fluids

NTA, WB, and TEM confirmed the presence of exosomes in VH. NTA results exhibited a high percentage (more than 70%) of 30 to 150 nm particle size vesicles for all kinds of VH vesicles in both the PM and control groups. The concentration of vitreous exosomes was $6.4 \pm 6.6 \times 10^6$ particle/uL in the control group and $20.7 \pm 29.2 \times 10^6$ particle/uL in the PM group. Concentration of exosomes and the exosome vesicle ratio did not change significantly between the two groups (Supplementary Fig. S1). WB results showed that the exosomes of VH expressed typical exosomal proteins such as CD9, CD63, CD81, and TSG101, but did not express mitochondrial marker cytochrome C and endoplasmic reticulum specific protein Calnexin, which confirmed the high purity of the exosomes (Fig. 2). The representative cup-like structure of exosomes could be observed in both control and PM groups (Fig. 3). The normal saline used to dilute VH samples did not affect the membrane integrity of the exosome and background. Exosomes extracted from VH were consistent with exosomes from other body fluids in characteristic proteins and morphology.

The Exosomes of VH in Patients With PM (AL >29 mm) Contain More RNA

RNA was further extracted from the samples and confirmed to have a high purity of exosomes. In order to understand the relationship between AL, exosome vesicle ratio (EVR), and average RNA content in VH of patients with PM, we compared the proportion of vitreous exosomes in total EV and the average content of RNA in total EV with different AL

Investigative Ophthalmology & Visual Science

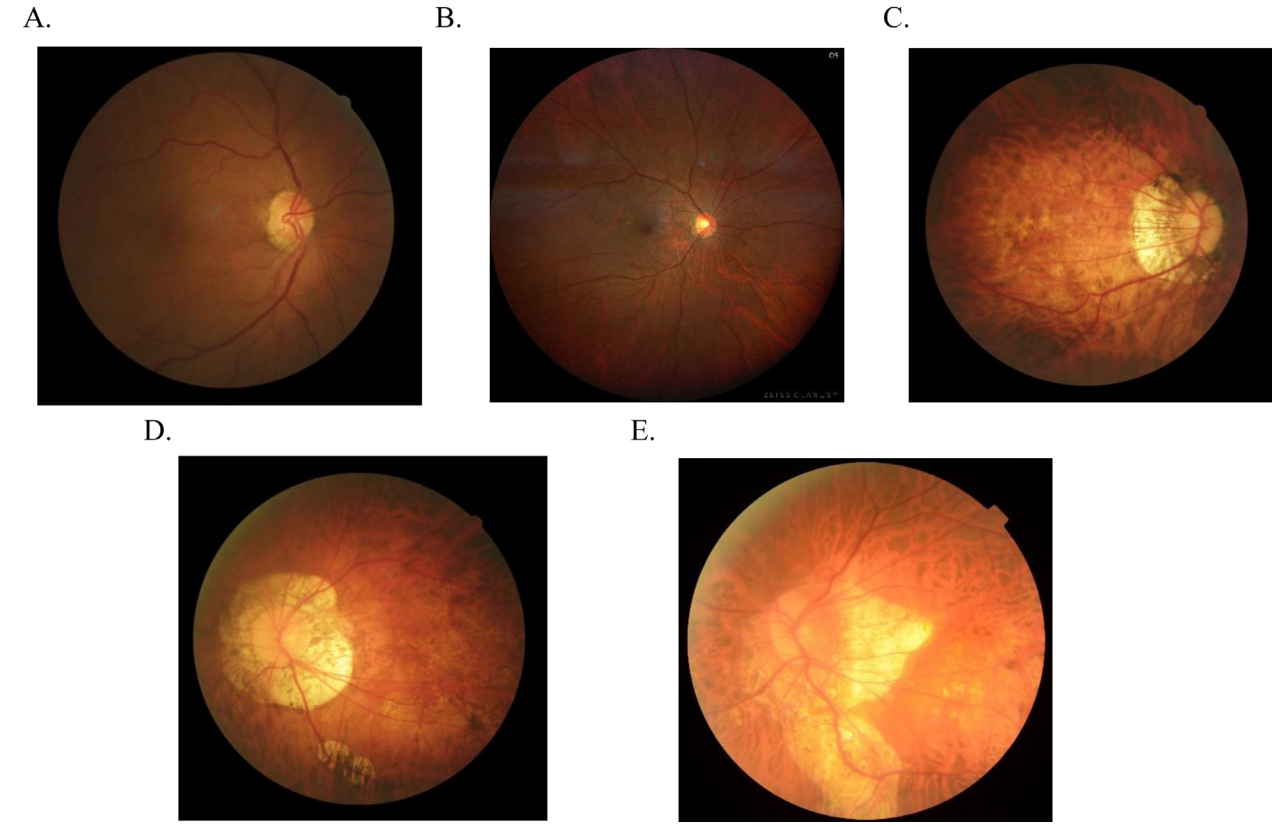

Figure 1. Fundus photographs of different grades of myopic maculopathy. (**A**) G0: no macular lesions; (**B**) G1: tessellated fundus; (**C**) G2: diffuse chorioretinal atrophy; (**D**) G3: patchy chorioretinal atrophy; (**E**) G4: macular atrophy.

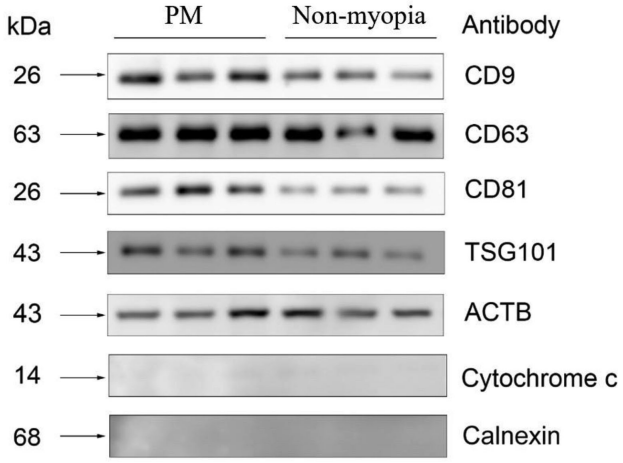

Figure 2. Western blot analysis of vitreous exosomes. The exosome in the vitreous for control and PM patients were positive for exosomal markers CD9, CD63, CD81, and TSG101. High purity of vitreous exosomes was confirmed using the following organelle markers: cytochrome c (mitochondria), and calnexin (endoplasmic reticulum).

of eyes (Table 2). We found that the EVR was consistent in patients with different eye AL. However, the average content of RNA per vesicle was higher in patients with eye AL of more than 29 mm (although failed to cross the threshold of classical statistical significance at 0.05), which suggests that vitreous exosomes may undertake more RNA transport tasks when AL reaches above 29 mm.

The myopia maculopathy classification and grading system consider G2 and upper maculopathy atrophy levels as PM.[13] In this study, we found that when the eye AL reaches 29 mm, the myopia maculopathy grade is likely to be G2 and greater. In other words, patients with AL greater than 29 mm are more likely to suffer from PM complications.

Exosomes From VH Were Rich in MicroRNAs

To further explore the composition and expression of RNA in VH exosomes of patients with PM, samples with RNA content >1 ng were selected (6 in the control group and 12 in the PM group. Patients' information can be obtained from Supplementary Table S1). After correlation analysis between the two groups, the microRNA composition of P-20 (G1) was found to resemble that of the control group (Fig. 4). Because G1 is not considered PM in the International Myopic Maculopathy Classification, the sample was removed in the subsequent DEM analysis.

Progression can be found in 63.7% of eyes with G2 myopic maculopathy and in greater than 97.4% of eyes with G3 and G4 myopic maculopathy after an 18-year follow-up.[1] That means G2 myopic maculopathy may to some extent be capable of slowing down the progression than the G3 and upper degree of myopic maculopathy, even though most of the choroid layer is absent in G2 myopic maculopathy.[13] In order to discern what leads to the development of the different myopia maculopathy stages, the PM group was further

Investigative Ophthalmology & Visual Science

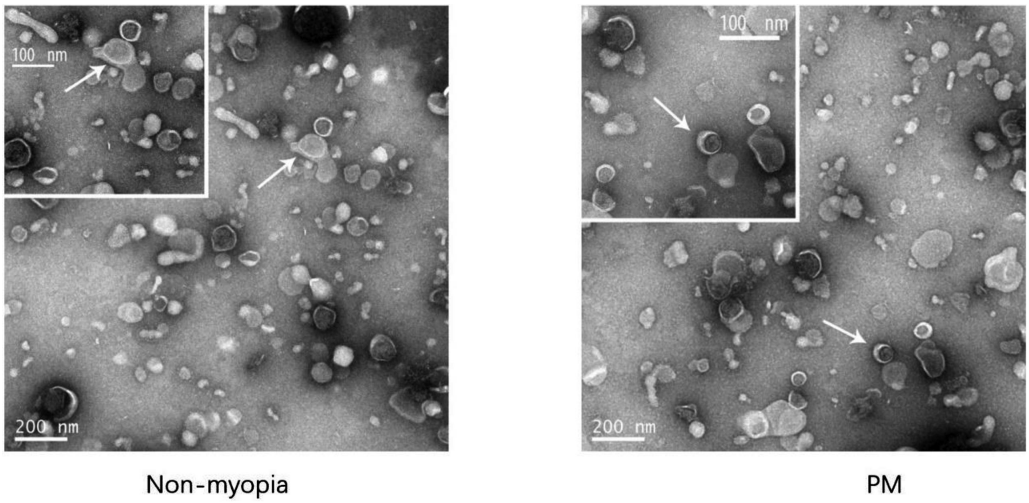

Figure 3. TEM images of vitreous exosomes. Exosomes indicated with *arrows*.

Table 2. Characteristics of Vitreous Samples From Patients With PM With Different AL

	22 < AL < 26.5	26.5 ≤ AL ≤ 29	AL > 29	*P* Value*
AL (mm)	23.2 ± 0.7	27.7 ± 0.5	31.2 ± 0.8	<0.001
Exosome vesicle ratio (%)	71.6 ± 12.8	71.1 ± 14.0	73.4 ± 5.4	0.888
RNA content per vesicle ($\times 10^{10}$ ng)	3.0 ± 5.1	0.5 ± 0.4	9.8 ± 15.6	0.076
G1	0	2 (50%)	0 (0%)	–
G2	0	1 (25%)	4 (36.4%)	–
G3	0	1 (25%)	6 (54.5%)	–
G4	0	0 (0%)	1 (9.1%)	–

* One-way analysis of variance. Welch's correction value was used when the variance was not uniform. Exosome vesicle ratio means the proportion of vitreous exosomes in total EV in VH. RNA content per vesicle refers to the average content of RNA in total EV.

divided into PM-L (G2) and PM-H (G3, G4) based on the different deterioration trends of myopic maculopathy.

Among all the detected microRNAs, the control group expressed 335, the PM-L group expressed 369, and the PM-H group expressed 383. Figure 5A shows the co-expressed and specific expressed microRNA numbers in control, PM-L, and PM-H samples. Average CPM was used to compare the total microRNA expression between groups (Fig. 5B). The control group possessed the lowest total microRNA number and expression. A 1.5-fold increase in total microRNA expression was observed in PM-L group. The PM-H group expressed the most kinds of microRNAs but had disproportional total microRNA expression that approaching to the control group indicated a downward-regulating trend in most microRNAs of the PM-H group.

Compared with the control group, several microRNAs increased for the ten top expressed microRNAs of the PM-L group, including *hsa-miR-423-5p*, *hsa-let-7b-5p*, *hsa-miR-99a-5p*, *hsa-miR-204-5p*, *hsa-miR-30d-5p*, and *hsa-miR-100-5p* (Fig. 6).

Differentially Expressed MicroRNA (DEM) Among PM-L, PM-H, and the Control Groups

DEM was analyzed between PM (L + H) versus control, PM-L versus control, PM-H versus control, and PM-H versus PM-L, and graphicly visualized by volcano plots (Figs. 7A–D). There were 95 DEMs upregulated in the PM-L versus control comparison and 85 DEMs downregulated in the PM-H versus PM-L comparison (Fig. 7E), which is consistent with the results mentioned above. DEMs of all comparisons can be obtained from Supplementary Table S2.

To study the possible reasons accounting for the tendency of deterioration in PM-H, microRNAs differently expressed between PM-H and PM-L groups were further examined to find out the possible pathways.

WGCNA Found Key MicroRNAs Related to Myopic Maculopathy

A WGCNA was conducted to explore the system-level functionality of the present microRNA groups and identify the most central genes within the module that relate most with myopic maculopathy.[14] To eliminate the influence of outlier samples in WGCNA, the results of correlation analysis (see Fig. 1) and sample clustering analysis were considered (Supplementary Fig. S2) and nine samples (3 samples of each group) were kept for the downstream analysis. Following preprocessing steps, 381 microRNAs were used to construct the co-expression network. Co-regulated microRNAs were grouped into a module based on similarities. Each module was assigned a color. A total of seven modules were identified (Fig. 8).

Among all the modules, the turquoise-colored module was associated most with the myopic maculopathy degree (Fig. 9). Other identified modules (age and gender) were not strongly associated with clinical characteristics ($P > 0.05$). The grey module represents background genes.

Investigative Ophthalmology & Visual Science

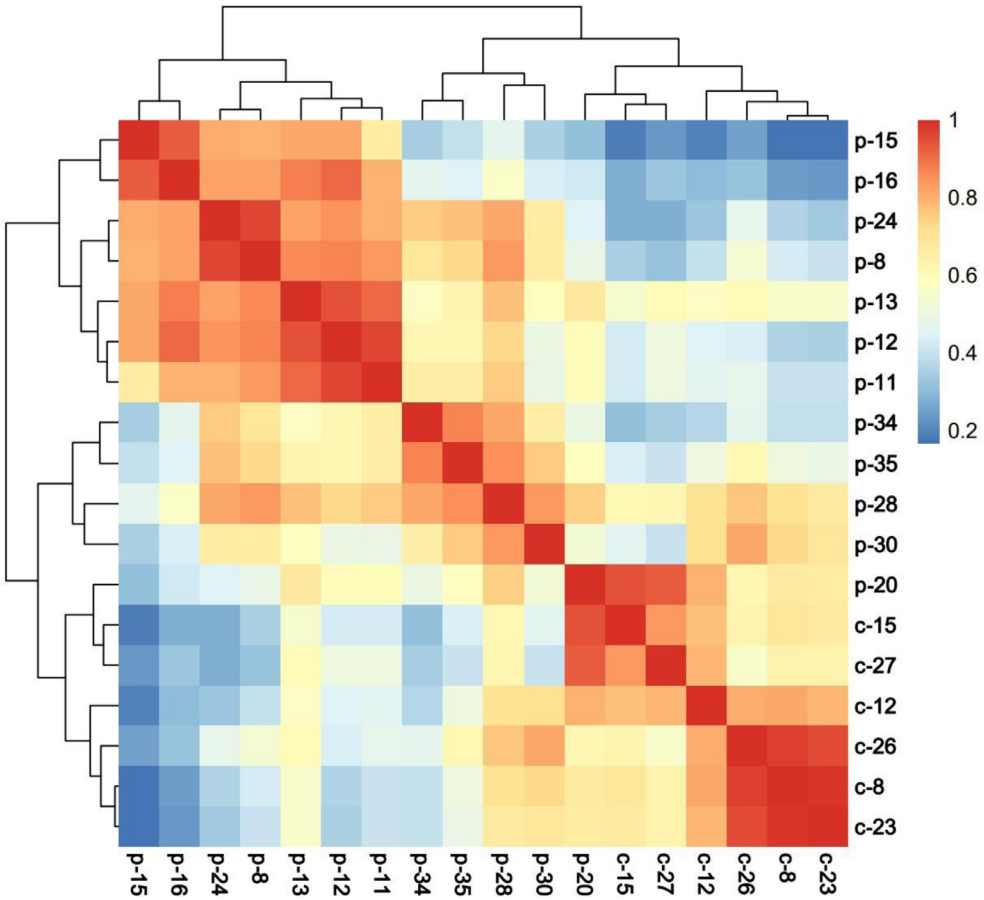

Figure 4. Correlation heatmap of all samples before differentially expressed microRNA analysis.

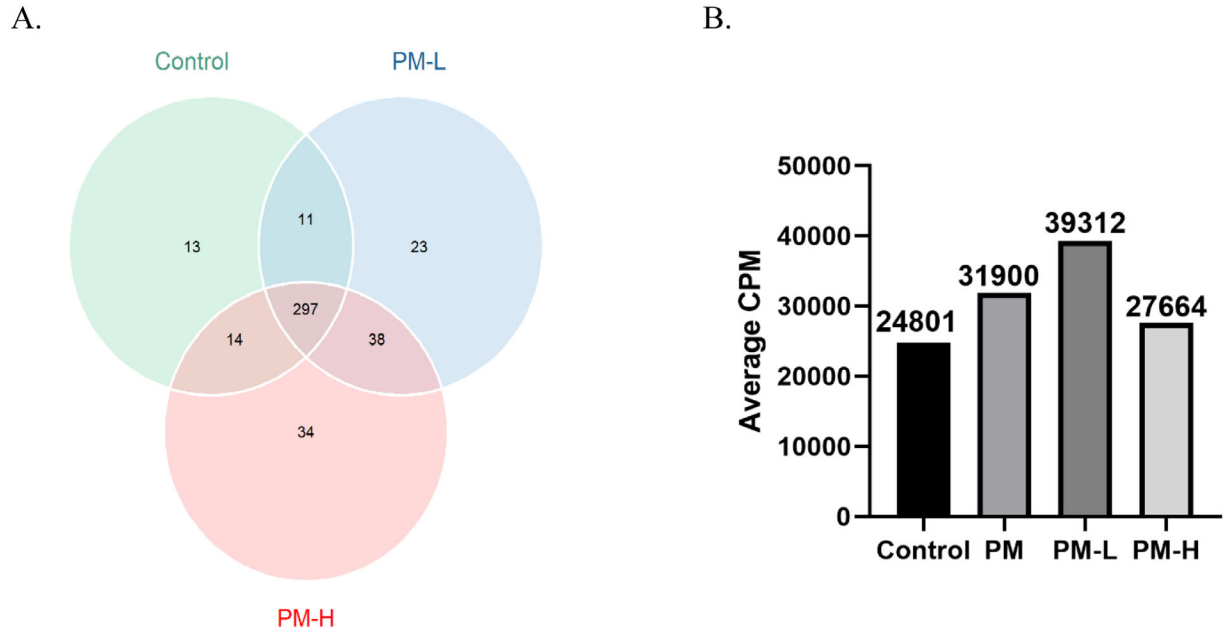

Figure 5. Overview characteristics of sample microRNAs. (**A**) Venn diagram of microRNA detection by next-generation sequencing (297 microRNAs expressed in all groups; 14 microRNAs only expressed in the control and PM-H groups; 38 microRNAs only expressed in the PM-H and PM-L groups; 11 microRNAs only expressed in the control and PM-L groups; 13 microRNAs specifically expressed in the control group; 34 microRNAs specifically expressed in the PM-H group; and 23 microRNAs specifically expressed in the PM-L group). (**B**) Average total microRNAs expression (CPM) of samples in the control, PM, PM-L, and PM-H groups.

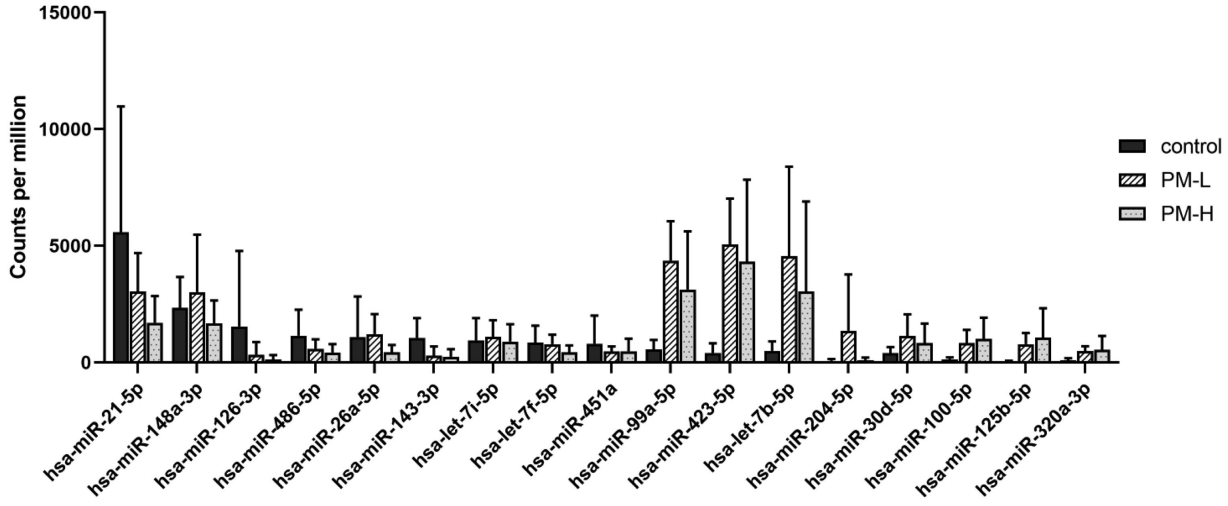

Figure 6. Frequency distribution of the ten most abundant mature microRNAs in the control group, PM-L group, and PM-H group as determined by next-generation sequencing.

The turquoise module negatively correlated with myopic maculopathy (r = −0.84, P = 0.004). In this module, 90 correlated microRNAs were extracted for further analysis. The strong relationship between myopic maculopathy and the turquoise module eigengene was determined by the relation between MM and GS (cor = 0.74, $P = 7.9e^{-17}$, Fig. 10).

Figure 11 shows a graphic depiction network of the turquoise-color module microRNAs. The key microRNAs (MM >0.9) in the turquoise module were considered as playing the central role in the module. The hub microRNAs were selected from the key microRNAs of the network and were highlighted, including *hsa-miR-25-3p*, *hsa-miR-143-3p*, *hsa-miR-192-5p*, and *hsa-miR-142-3p*. The individual result of each microRNA in the module can be found in Supplementary Table S3.

KEGG and GO Analysis of PM-H versus PM-L DEM and Hub MicroRNAs Found in WGCNA

All six upregulated and the top five downregulated microRNAs (*hsa-miR-204-5p*, *hsa-miR-26a-5p*, *hsa-miR-151a-3p*, *hsa-miR-204-3p*, and *hsa-miR-126-3p*) selected from the PM-H versus PM-L DEM and all four hub microRNAs found in WGCNA were used to conduct the KEGG and GO analysis. Only pathways with p.adjust (FDR) less than 0.05 were considered applicable to the analysis (ranked by FDR). Due to the low expression, the upregulated DEMs of PM-H versus PM-L may not be suitable for practical use as a prognosis biomarker, the results of which can be found in Supplementary Table S4 and S5. Figure 12 shows the top 20 KEGG and top 10 GO analysis results of the top 5 downregulated microRNAs selected from the PM-H versus PM-L DEM. The pathways that may participate in the progression of myopic maculopathy, including the KEGG pathway "Proteoglycans in cancer" and "Insulin resistance."

Figure 13 shows the KEGG and GO analysis results of the 4 hub microRNAs found in WGCNA. There were several pathways that may relate to myopic maculopathy. Such as the KEGG pathway: "Regulation of actin cytoskeleton" and "Proteoglycans in cancer."

Discussion

This Study Is a Novel Attempt to Use Vitreous Exosomes to Explore PM Maculopathy

Pathological myopia differs from high myopia in that it exhibits characteristic pathological changes in the posterior fundus. About 1% to 3% of Asians and 1% of Caucasians suffer from PM.[13] Myopia macular degeneration is the second most common cause of visual impairment and blindness.[15] VH contains the biological characteristic molecules of various retinal diseases[9] and has been used in research of retinal diseases like age-related macular degeneration (AMD), diabetic retinal disease, and glaucoma.[16] Exosomes have been confirmed to exist in VH and might play an important role in preventing the process of retinal atrophy.[8,17] Vitreous bodies are anatomically close to the retina, and the contained exosomes may be primarily secreted from the retina and adjacent tissues. Therefore, the components of vitreous exosomes in patients with PM can indirectly reflect the state of their myopia maculopathy.

Previous studies have extracted vitreous exosomes from donated eye samples. This study is the first to have extracted exosomes from a single vitreous sample which was collected from patients undergoing retinal surgery. After multiple attempts, we did not choose to gather vitreous samples in the usual way, but rather collected samples with the intraocular saline infusion prior to the surgery. Although diluting the VH, the intraocular perfusion can reduce sampling interference in retinal surgery for patients and obtain the maximum amount of VH. The recognized gold standard method – ultracentrifugation,[18] then reduced the effect of saline dilution to the maximum extent. The NTA, WB, and TEM analysis all demonstrated that high-purity 30 to 150 nm vesicles were obtained from the diluted VH samples.

The Vitreous Exosome Contains MicroRNAs Highly Related to the Progression of Pathological Myopic Maculopathy and AL Elongation

Previous researchers have studied the vitreous profile of microRNAs in high myopic eyes without differentiating the

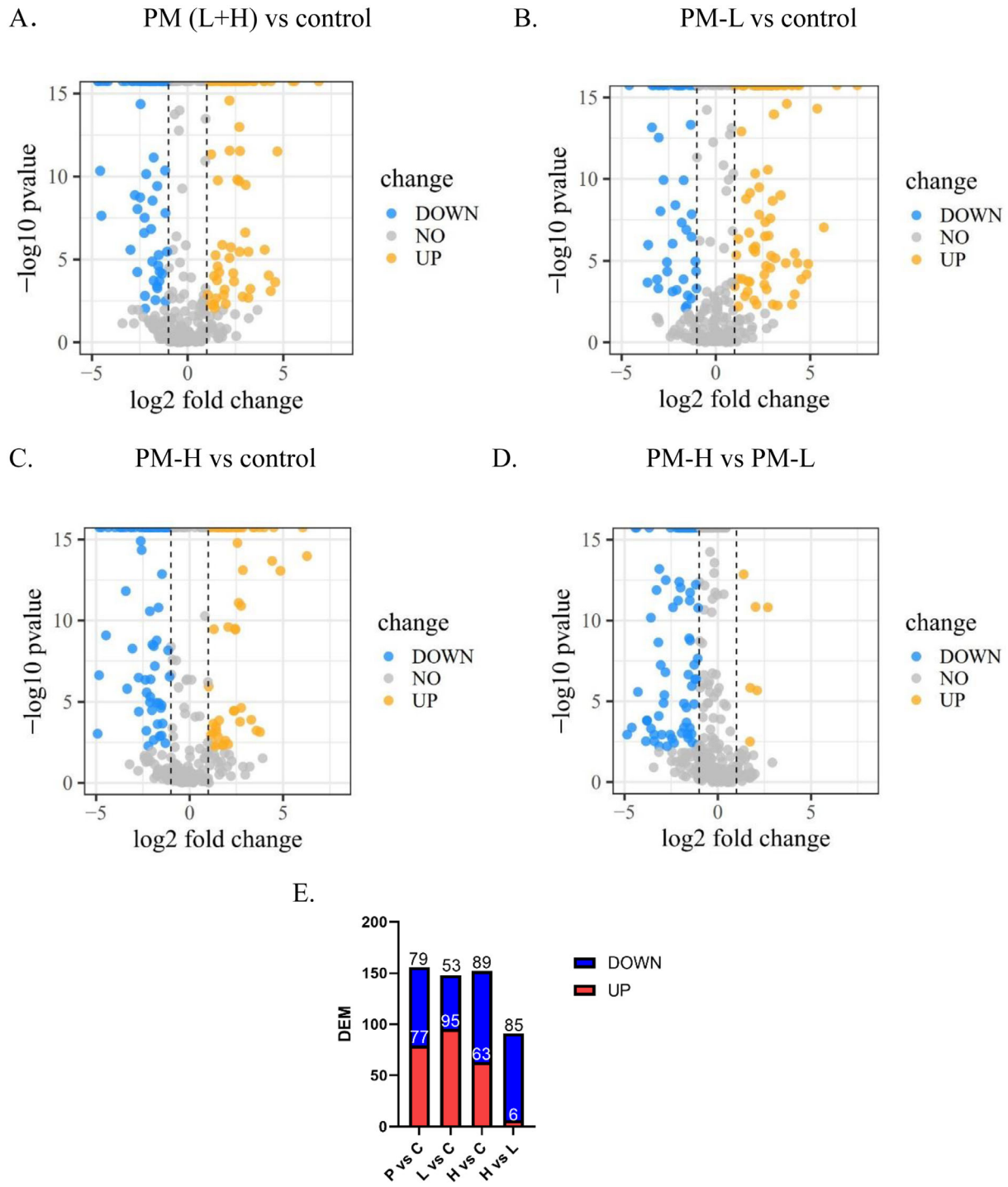

Figure 7. Overview of characteristics of differentiated expression microRNAs (DEMs). (**A**) Volcano plot of DEMs between PM (L + H) versus the control groups. (**B**) Volcano plot of DEMs between the PM-L versus the control groups. (**C**) Volcano plot of DEMs between the PM-H versus the control groups. (**D**) Volcano plot of DEMs between the PM-H versus the PM-L groups. (**E**) The number of upregulated and downregulated DEMs between the PM (L + H) versus the control group, PM-L versus the control group, PM-H versus the control group, and PM-H versus the PM-L group.

degree of myopic maculopathy. This approach has overlooked essential messages with upregulation of exosomal microRNAs in PM-L versus control and the significant downregulation of exosomal microRNAs in PM-H (G3 and G4) versus PM-L observed in the present cohort.

This research not only explored the exosomal microRNAs that persistently alter in the progression of myopic maculopathy and AL using WGCNA but also discerned the most abundant exosomal microRNAs accounting for the deteriorating tendency of G3 and G4 myopic maculopathy through differentially expressed analysis of microRNAs. The KEGG

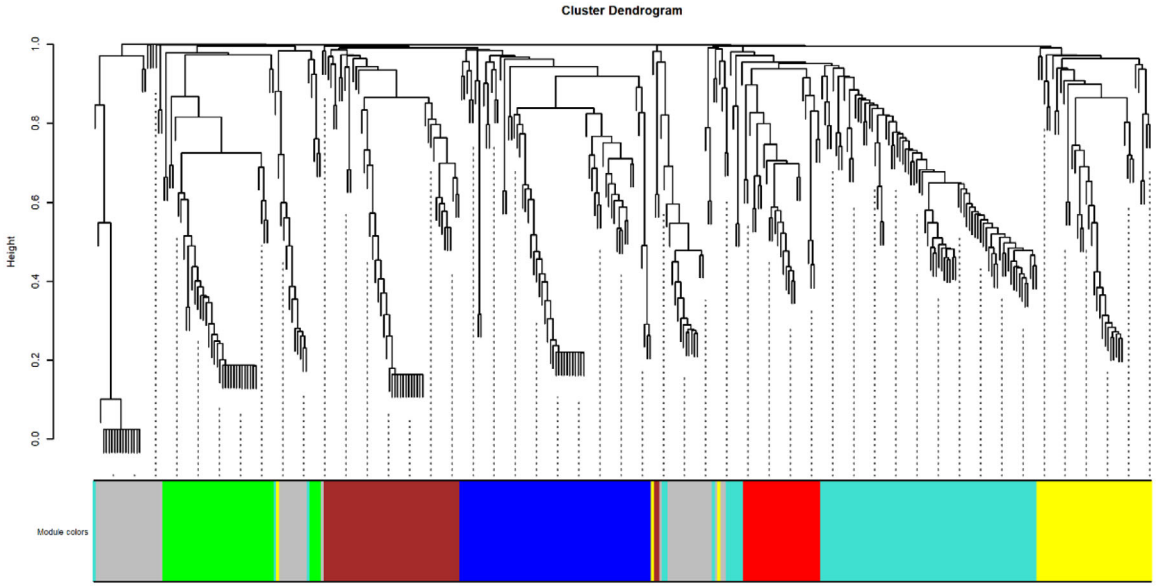

Figure 8. Gene dendrogram of the co-expression modules relating to external traits.

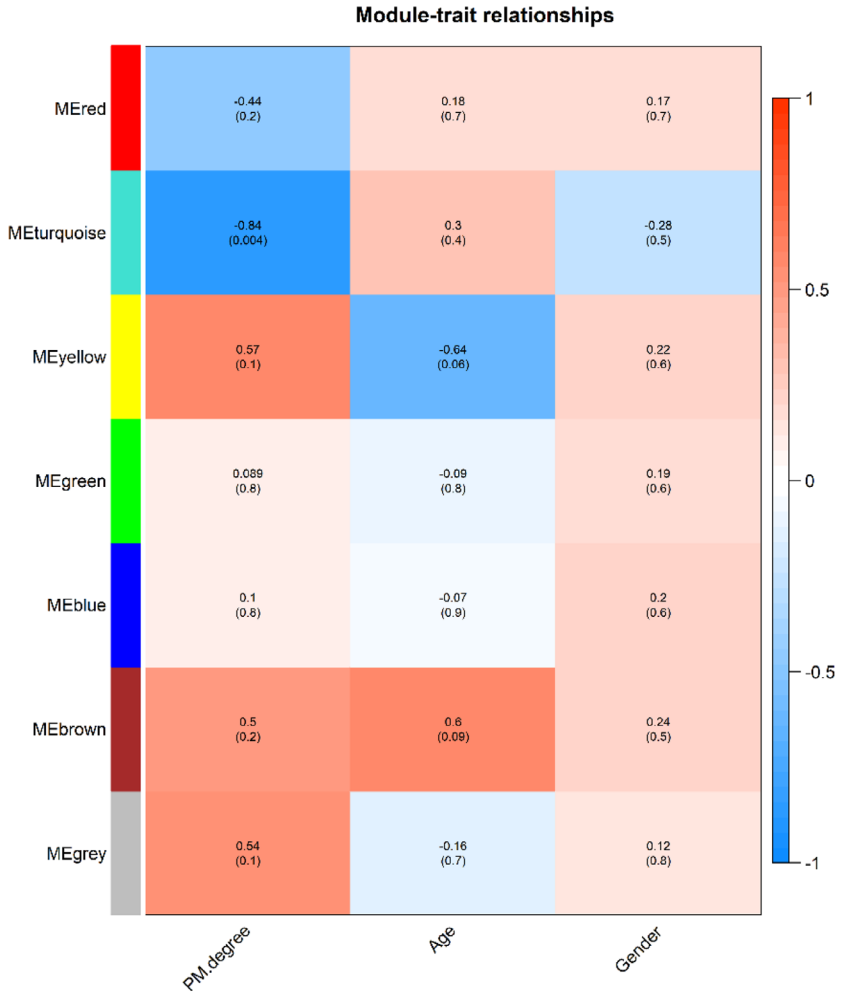

Figure 9. Module-trait relationships of myopic maculopathy (each cell contains the corresponding correlation and *P* value).

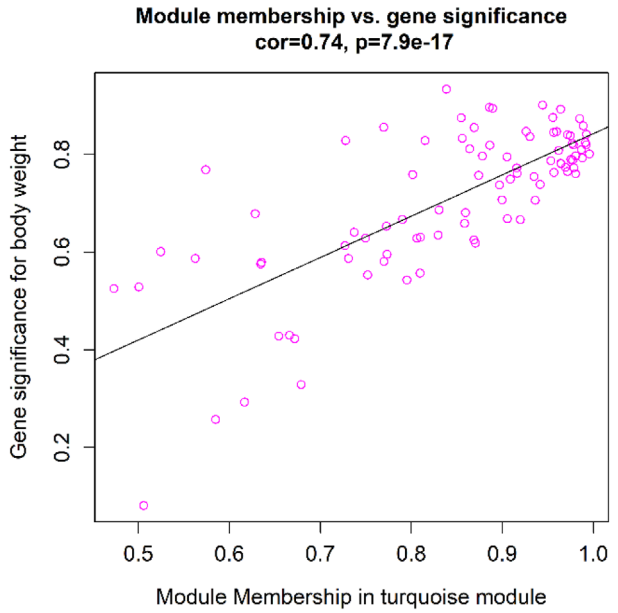

Figure 10. The relation between Module Membership and Gene Significance in myopic maculopathy, which reflected the strong relationship between myopic maculopathy and the turquoise module eigengene.

and GO pathway analysis was also conducted in the comparison of PM (L + H) versus control and PM-L versus control (Supplementary Tables S4, S5). Co-existence of the protecting effects and damaging effects in PM-L exosomal microRNAs prevented further conclusions in this study: further research is needed to understand the complicated function of exosomal microRNAs in PM-L. However, with the help of WGCNA, key threads functioning throughout myopic maculopathy could be found.

Vitreous Exosomal *miR-143-3p* and *miR-145-5p* May Participate in the Growth of AL and the Progression of the Myopic Maculopathy

As shown in Figure 6, *miR-143-3p* was one of the most abundant microRNAs in the vitreous exosome of control eyes. The downregulation trend observed in this study (Table 3) is also consistent with the microRNA expression characteristics of other tissue/fluid in the eye during myopia (Table 4). The change of *miR-143-3p* and other key microRNAs was not found in the differentially expressed analysis of microRNAs in VH obtained from patients with high myopia[19] indicating the more stable expression of exosomal microRNAs in the VH. Another study that detected the retinal microRNAs profile after 10 days of visual formed deprivation showed the down-regulation of mmu-miR-143-3p, mmu-miR-142-3p, and mmu-miR-145-5p.[20] It suggested that the three microRNAs may play a role in the retinal defocus signal transmission in early myopia formation. Then, *miR-143-3p* and *miR-145-5p* kept on functioning throughout the progression of myopic maculopathy (perhaps through the elongation of the AL, which was also negatively correlated with the turquoise module, see Supplementary Figs. S4, S5). The downregulated trend of the expression of *hsa-miR-143-3p* in PM-H versus PM-L did not reach the significance and *hsa-miR-143-3p* may not play the most important role in late phase myopia maculopathy progression. However, the trend was in line with no significant difference in AL between PM-H versus PM-L (Supplementary Table S1, $p = 0.119$), which add a clue for the possible relation of *hsa-miR-143-3p* and AL. *MiR-143* directly targeted IGF-1Rβ and *miR-145* directly targeted IRS-1 in vascular smooth muscle cells.[21] The 3′UTRs of IGF-2R were also targeted by *miR-143-3p*, which brought about the obesity insulin resistance.[22] The intravitreal injection of insulin and insulin like growth factor (IGF) can cause AL growth in chicks.[23,24] The down-regulation of *miR-143* and *miR-145* may increase the

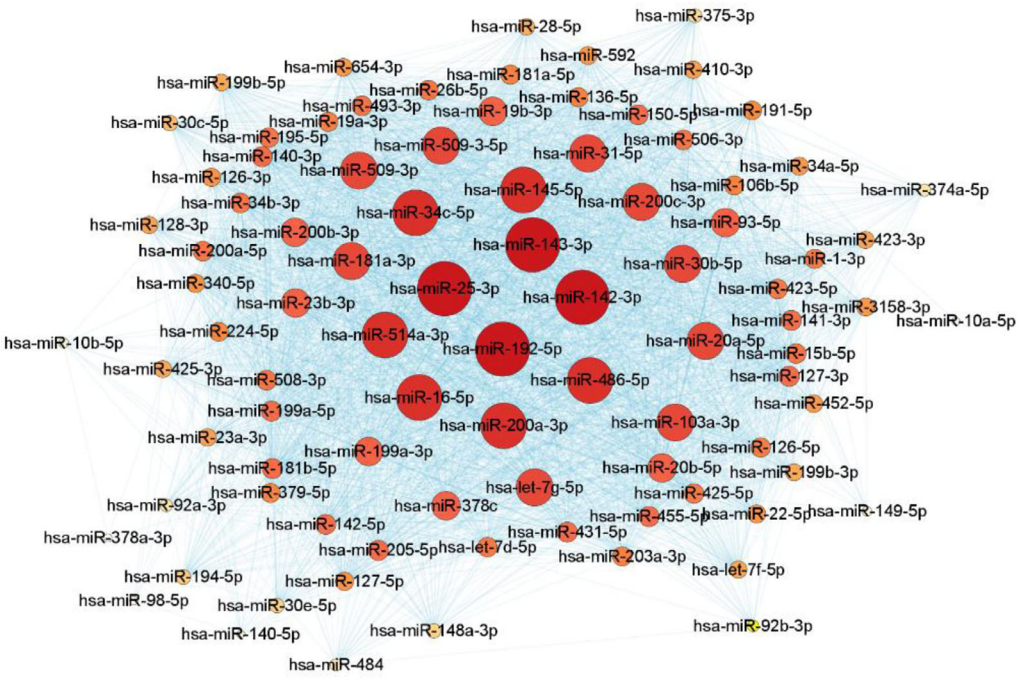

Figure 11. Graphic depiction of the turquoise-color module. The hub microRNAs of the network were highlighted (*hsa-miR-25-3p*, *hsa-miR-143-3p*, *has-miR-192-5p*, and *hsa-miR-142-3p*), the redder and bigger the spot, the higher note degree score of the corresponding gene.

Figure 12. The top 20 enriched KEGG pathways and the top 10 enriched GO-BP (green), CC (orange), and MF (blue) pathways (ranked by FDR) of the PM-H versus the PM-L DEMs (downregulated).

expression of the receptor of IGF, thus activating the downstream of the insulin resistance pathway and resulting in AL growth.

The *miR-143-3p* and *miR-145-5p* may also participate in the progression of myopic maculopathy through the cytoskeletal remodeling of retinal vascular smooth muscle (VSMCs) after vascular injuries. Neointimal formation of cardiac vessels significantly decreases in both miR-143 KO and miR-145 KO mice.[26,27] Choroid blood supply the outer retina and the thinning of the choroid may result in the ischemic injury of retinal vessels and the neuron. The reduced exosomal *miR-143* and *miR-145* prevent the responsiveness of smooth muscle cells to injury and deteriorate myopic maculopathy.

There are many questions that need to be explored, including the recipient cell of vitreous exosomal *miR-143* and *miR-145* and their function in AL; the asynchronized expression of *miR-142-3p* and other key microRNAs in vitreous exosome and aqueous humor,[25] considering the upregulation of *miR-142-3p* has been observed to reduce collagen I in sclera fibroblasts, indicating a different function of *miR-142-3p* in vitreous exosomes. The expression characteristics and possible function in the retina, as well as exosome of all key microRNAs of published researches, are summarized in Supplementary Table S6.

The Most Abundant Downregulated Vitreous Exosomal DEMs of PM-H Versus PM-L Possess Essential Functions in Retina

The prognosis of myopic maculopathy in PM-H (G3, G4) is much worse than in PM-L (G2). A series of downregulated vitreous exosomal microRNAs that may account for the difference were found. The top five microRNAs of DEM of PM-H versus PM-L were either possessing protective ability in the retina or play an essential role in the maintenance of the retina.

Investigative Ophthalmology & Visual Science

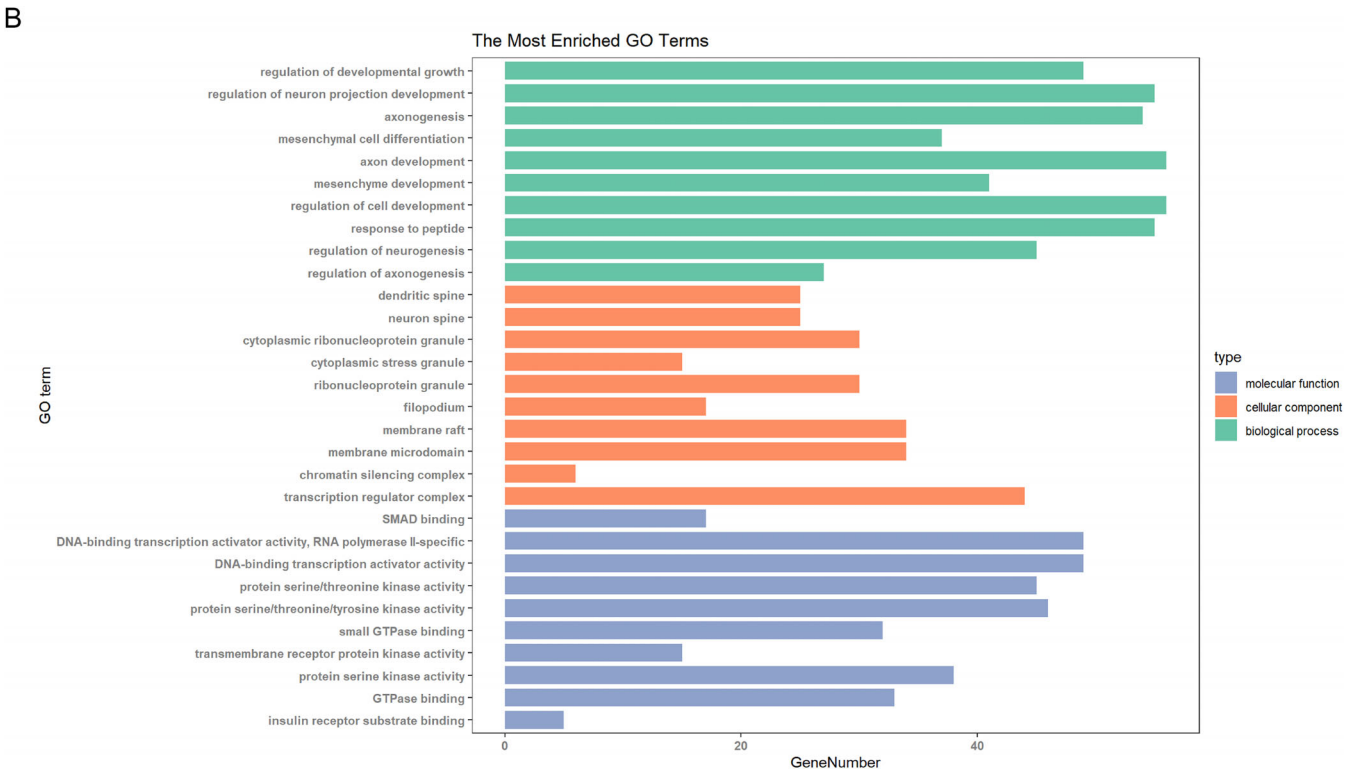

Figure 12. Continued

Table 3. Integrated Results* of the Selected Exosomal MicroRNAs

microRNA	Module Color	MM Turquoise	PM (L + H) Versus C.log2FC	PM-L Versus C.log2FC	PM-H Versus C.log2FC	PM-H Versus PM-L.log2FC	PM (L + H) Versus C	PM-L Versus C	PM-H Versus C	PM-H Versus PM-L
hsa-miR-25-3p	Turquoise	0.996	−1.489	−1.099	−1.770	−0.671	Down	Down	Down	No
hsa-miR-143-3p	Turquoise	0.993	−2.009	−1.844	−2.112	−0.267	Down	Down	Down	No
hsa-miR-192-5p	Turquoise	0.989	−1.972	−1.942	−1.989	−0.046	Down	Down	Down	No
hsa-miR-142-3p	Turquoise	0.980	−1.802	−1.937	−1.731	0.207	Down	Down	Down	No
PM-H vs L top5										
hsa-miR-204-5p	Grey	−0.167	3.149	4.423	0.745	−3.678	Up	Up	No	Down
hsa-miR-26a-5p	Blue	−0.165	−0.603	0.152	−1.322	−1.474	No	No	Down	Down
hsa-miR-151a-3p	Blue	−0.042	0.600	1.470	−0.325	−1.795	No	Up	No	Down
hsa-miR-204-3p	Green	−0.223	1.502	2.210	0.853	−1.358	Up	Up	No	Down
hsa-miR-126-3p	Turquoise	0.770	−2.902	−2.190	−3.556	−1.366	Down	Down	Down	Down

* To confirm the downregulated trend of the hub microRNAs in larger sample size, the results of WGCNA (9 samples) were integrated with differentially expressed analysis (all qualified 17 samples) mentioned earlier.

Table 4. Integrated Key MicroRNAs Expression Characteristics in Vitreous Exosome and Other Tissue/Fluid During Myopia

Gene Name	Vitreous Exosome	Vitreous Humor[19]	Retina[20]	Aqueous Humor[25]
Species	Homo sapiens	Homo sapiens	Mus culus	Homo sapiens
miR-142-3p	Down	/	Down	Up
miR-181a-5p	Down	/	/	Up
miR-127-3p	Down	/	/	Up
miR-16-5p	Down	/	/	Up
miR-142-5p	Down	/	/	Up
miR-150-5p	Down	/	/	Up
miR-200a-3p	Down	Down	/	/
miR-143-3p	Down	/	Down	Down
miR-145-5p	Down	/	Down	Down

Figure 13. The top 20 enriched KEGG pathways and the top 10 enriched GO-BP (green), CC (orange), and MF (blue) pathways (ranked by FDR) of the hub microRNAs found in WGCNA.

The *miR-204* is one of the most highly expressed microRNAs in the RPE layer. RPE cell dysfunction, in which *miR-204* is a key player, results in photoreceptor degeneration. In this way, *miR-204* performs critical functions during retinal development and maintenance.[28,29] The aberration of *miR-204* may reflect the irreversible changes of the retina.

The miR-126-5p is expressed both in endothelial cells and in retinal ganglion cells (RGCs). The miR-126-5p expressed by RGCs has a protective function toward retinal endothelial cells and promotes their survival.[30] *MiR-26a* was downregulated in patients with diabetes with retinal neurodegeneration. Intravitreal administration of *miR-26a* mimics can attenuate damage of RGCs caused by diabetes.[31] Decreased quantity of these microRNAs in vitreous exosome may aggravate myopic maculopathy through the process mentioned above.

The vitreous exosomal DEMs of PM-H versus PM-L also took part in the insulin resistance pathway, which relates to the formation of myopia.[32] The predicted targets were graphically shown in Figure 14. A network of the predicted microRNA-mRNAs in the "Proteoglycans in cancer" pathway was also conducted (Supplementary Fig. S6). The abnormal proteoglycans metabolisms in the retina may influence the extracellular matrix and promote the epithelial-mesenchymal transition of retinal epithelium cells.

Deficiencies and Limitations of this Study

The deficiency of this study is the limited number of qualified samples for sequencing analysis (total RNA >1 ng). The exosomes contain not only RNA; there are also protein polypeptides and lipids constituting the exosomes' composi-

Investigative Ophthalmology & Visual Science

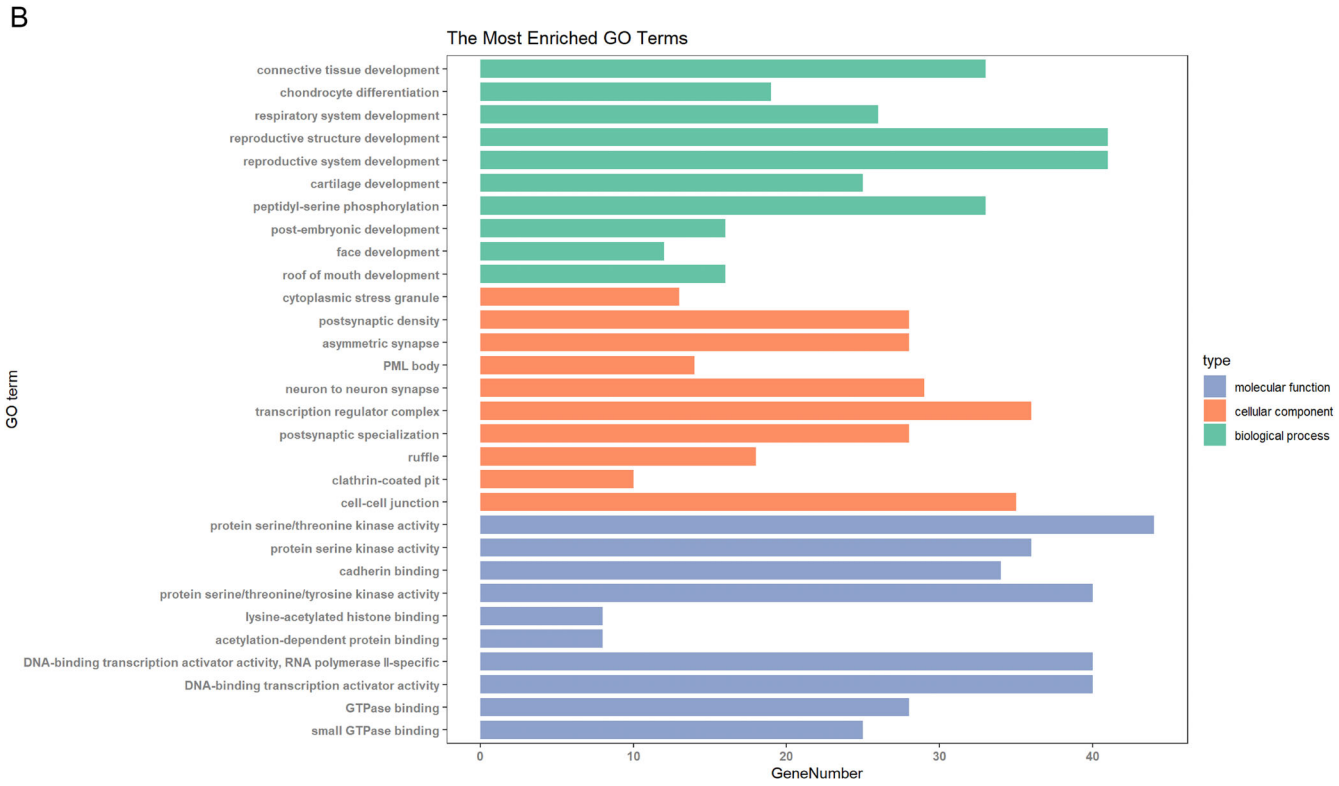

Figure 13. Continued

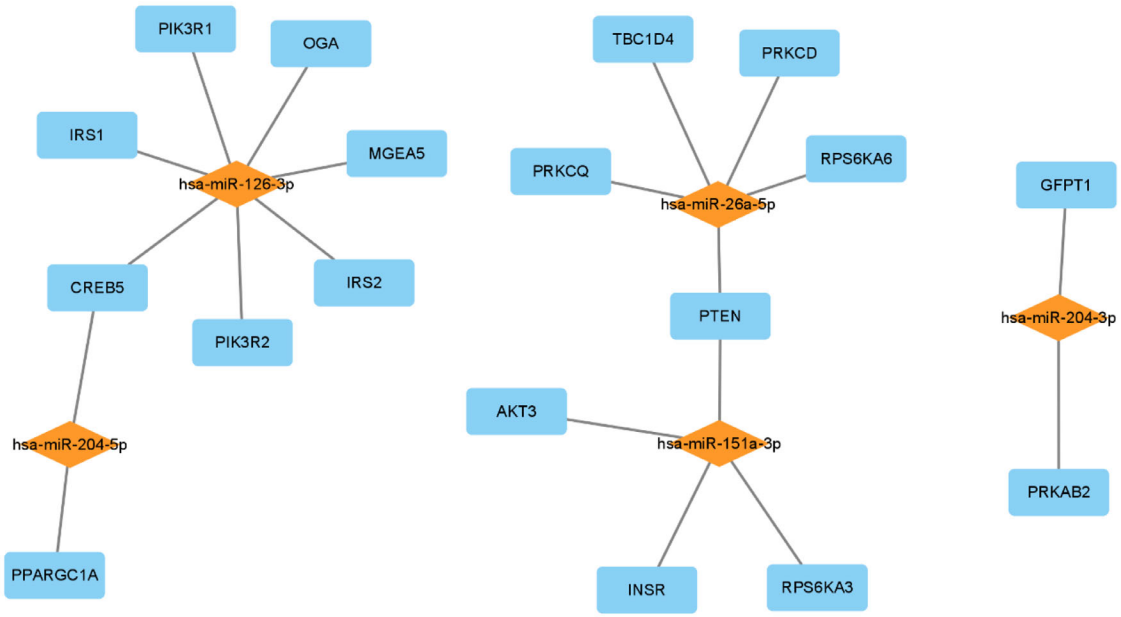

Figure 14. Network of the predicted microRNA-mRNAs in insulin resistance.

tions in some samples. Therefore, other components of vitreous exosomes should be further explored. Similarly, due to the small number of qualified samples, microRNA expression verification is not available. We will explore better sampling and extracting methods in future studies to obtain vitreous exosome samples with higher RNA content. Table 4 shows the consistent and inconsistent transformations of PM vitreous exosomal microRNAs and aqueous humor in high myopia. Without determining the myopic maculopathy degree of high myopia, it is hard to tell whether the microRNAs in aqueous humor possesses the similar function with exosomal microRNAs in vitreous. The research did not detect the corresponding aqueous exosomal microRNAs and further research is needed.

Investigative Ophthalmology & Visual Science

Conclusions

This research extracted exosomes from VH of surgery-treated eyes from patients with PM and controls to study the progression of myopic maculopathy for the first time. The presence and high purity of vitreous exosomes were confirmed by NTA, WB, and TEM. RNA was extracted from exosomes of VH.

The hub microRNAs and DEM discovered in this study may participate in the insulin resistance of AL growth and thus promote the progression of myopic maculopathy. Notably, vitreous exosomal *miR-143-3p* and *miR-145-5p* can become biomarkers for patients with PM, and the vitreous exosomal DEM associate with PM-H may represent alarming signals of myopic maculopathy deterioration.

Acknowledgments

Funded by the National Natural Science Foundation of China (No.81870660) and Science and the Technology Innovation Action Plan of Shanghai Science and Technology Commission (No. 22Y11910500) to L. Chen.

Disclosure: **J. You**, None; **Q. Wu**, None; **G. Xu**, None; **C. Gu**, None; **E. Allen**, None; **T. Zhu**, None; **L. Chen**, None

References

1. Fang Y, Yokoi T, Nagaoka N, et al. Progression of Myopic Maculopathy during 18-Year Follow-up. *Ophthalmology*. 2018;125:863–877.
2. Flitcroft DI, He M, Jonas JB, et al. IMI - Defining and Classifying Myopia: A Proposed Set of Standards for Clinical and Epidemiologic Studies. *Invest Ophthalmol Vis Sci*. 2019;60:M20–M30.
3. Ohno-Matsui K, Lai TY, Lai CC, Cheung CM. Updates of pathologic myopia. *Prog Retin Eye Res*. 2016;52:156–187.
4. Kalluri R, LeBleu VS. The biology, function, and biomedical applications of exosomes. *Science*. 2020;367:eaau6977.
5. Hsu KS, Otsu W, Li Y, et al. CLIC4 regulates late endosomal trafficking and matrix degradation activity of MMP14 at focal adhesions in RPE cells. *Sci Rep*. 2019;9:12247.
6. Tsai CY, Chen CT, Lin CH, et al. Proteomic analysis of Exosomes derived from the Aqueous Humor of Myopia Patients. *Int J Med Sci*. 2021;18:2023–2029,
7. Deng CL, Hu CB, Ling ST, et al. Photoreceptor protection by mesenchymal stem cell transplantation identifies exosomal MiR-21 as a therapeutic for retinal degeneration. *Cell Death Differ*. 2021;28:1041–1061.
8. Ke Y, Fan X, Hao R, et al. Human embryonic stem cell-derived extracellular vesicles alleviate retinal degeneration by upregulating Oct4 to promote retinal Muller cell retrodifferentiation via HSP90. *Stem Cell Res Ther*. 2021;12:21.
9. Zhao Y, Weber SR, Lease J, et al. Liquid Biopsy of Vitreous Reveals an Abundant Vesicle Population Consistent With the Size and Morphology of Exosomes. *Transl Vis Sci Technol*. 2018;7:6.
10. Ohno-Matsui K, Kawasaki R, Jonas JB, et al. International photographic classification and grading system for myopic maculopathy. *Am J Ophthalmol*. 2015;159:877–883.e877.
11. Ma Z, Castillo-González C, Wang Z, et al. Arabidopsis Serrate Coordinates Histone Methyltransferases ATXR5/6 and RNA Processing Factor RDR6 to Regulate Transposon Expression. *Dev Cell*. 2018;45:769–784.e766.
12. Yepes S, López R, Andrade RE, Rodriguez-Urrego López-Kleine L, Torres MM. Co-expressed miRNAs in gastric adenocarcinoma. *Genomics*. 2016;108:93–101.
13. Ohno-Matsui K, Wu PC, Yamashiro K, et al. IMI Pathologic Myopia. *Invest Ophthalmol Vis Sci*. 2021;62:5.
14. Langfelder P, Horvath S. WGCNA: an R package for weighted correlation network analysis. *BMC Bioinformatics*. 2008;9:559.
15. Xu L, Wang Y, Li Y, et al. Causes of blindness and visual impairment in urban and rural areas in Beijing: the Beijing Eye Study. *Ophthalmology*. 2006;113:1134. e1131-1111.
16. Klingeborn MEA. Roles of exosomes in the normal and diseased eye. *Prog Retin Eye Res*. 2017;59:158–177.
17. Bian B, Zhao C, He X, et al. Exosomes derived from neural progenitor cells preserve photoreceptors during retinal degeneration by inactivating microglia. *J Extracell Vesicles*. 2020;9:1748931.
18. Jeppesen DK, Hvam ML, Primdahl-Bengtson , et al. Comparative analysis of discrete exosome fractions obtained by differential centrifugation. *J Extracell Vesicles*. 2014;3:25011.
19. Ando Y, Keino H, Inoue M, et al. Circulating Vitreous microRNA as Possible Biomarker in High Myopic Eyes with Macular Hole. *Int J Mol Sci*. 2022;23:3647.
20. Lan S, Albinsson S. Regulation of IRS-1, insulin signaling and glucose uptake by miR-143/145 in vascular smooth muscle cells. *Biochem Biophys Res Commun*. 2020;529:119–125.
21. Xihua L, Shengjie T, Weiwei G, et al. Circulating miR-143-3p inhibition protects against insulin resistance in Metabolic Syndrome via targeting of the insulin-like growth factor 2 receptor. *Transl Res*. 2019;205:33–43.
22. Feldkaemper MP, Neacsu I, Schaeffel F. Insulin acts as a powerful stimulator of axial myopia in chicks. *Invest Ophthalmol Vis Sci*. 2009;50:13–23.
23. Ritchey ER, Zelinka CP, Tang J, Liu J, Fischer AJ. The combination of IGF1 and FGF2 and the induction of excessive ocular growth and extreme myopia. *Exp Eye Res*. 2012;99:1–16.
24. Tkatchenko AV, Luo X, Tkatchenko TV, et al. Large-Scale microRNA Expression Profiling Identifies Putative Retinal miRNA-mRNA Signaling Pathways Underlying Form-Deprivation Myopia in Mice. *PLoS One*. 2016;11(9):e0162541.
25. Zhu Y, Li W, Zhu D, Zhou J. microRNA profiling in the aqueous humor of highly myopic eyes using next generation sequencing. *Exp Eye Res*. 2020;195:108034.
26. Xin M, Small EM, Sutherland LB, et al. MicroRNAs miR-143 and miR-145 modulate cytoskeletal dynamics and responsiveness of smooth muscle cells to injury. *Genes Dev*. 2009;23:2166–2178.
27. Cordes KR, Sheehy NT, White MP, et al. miR-145 and miR-143 regulate smooth muscle cell fate and plasticity. *Nature*. 2009;460:705–710.
28. Bereimipour A, Najafi H, Mirsane ES, Moradi S, Satarian L. Roles of miR-204 in retinal development and maintenance. *Exp Cell Res*. 2021;406:112737.
29. Bereimipour A, Satarian L, Taleahmad S. Investigation of Key Signaling Pathways Associating miR-204 and Common Retinopathies. *Biomed Res Int*. 2021;2021:5568113.
30. Villain G, Poissonnier L, Noueihed B, et al. miR-126-5p promotes retinal endothelial cell survival through SetD5 regulation in neurons. *Development*. 2018;145: dev156232.
31. Shi R, Liu DD, Cao Y, Xue YS. microRNA-26a-5p Prevents Retinal Neuronal Cell Death in Diabetic Mice by Targeting PTEN. *Curr Eye Res*. 2022;47:409–417.
32. Galvis V, López-Jaramillo P, Tello A, et al. Is myopia another clinical manifestation of insulin resistance? *Med Hypotheses*. 2016;90:32–40.